MODELING OF HYDROGASIFICATION OF A SINGLE LIGNITE CHAR PARTICLE

G.P.Sakellaropoulos, G.Skodras, S.P.Kaldis,
G.G.Stavropoulos and P.S.Kokorotsikos

Department of Chemical Engineering and
Chemical Process Engineering Research Institute
Aristotle University of Thessaloniki
Thessaloniki, Greece 54006

INTRODUCTION

Gasification, devolatilization, combustion and other coal conversion processes are quite complex, involving numerous, not well defined reactions, and simultaneous physical structure transformations. In order to describe these phenomena, several efforts have been reported, based either on empirical kinetic expressions (1-5) or on theoretical models (6-12). In the former, rate expressions are given in terms of volatile species, residual and active carbon, and reactant gas concentration or pressure. Theoretical models attempt to couple reaction rates with mass and heat transfer processes. The various models, however, differ significantly from each other, because of the diversity of the chemical and physical phenomena which they describe (e.g. pyrolysis, combustion, steam gasification etc) and the differences in assumptions and simplifications involved in each one.

Fast coal processes, such as oxygen combustion, rapid pyrolysis and devolatilization are usually considered to proceed via a shrinking core model, either isothermally or non-isothermally (6-11). Mass transport limitations are often assumed to occur within a reacted shell, surrounding a coal particle (6-7). The pore structure of the reacting particles is considered unchanged, in most of these models (6-9), although the effect of pore size distribution has been examined (8).

Structural variations of coal with reaction time have been included in few models, such as in hydropyrolysis of softening coals (10), in coal-oxygen reactions (11) and in char gasification (12). In a comprehensive analysis of coal combustion models, Sotirchos and Amundson (11) considered only the macropores of coal. Thus, local conversion and pore structure depended only on the thermal gradients at various total conversions. Lee at al. (12) developed a char gasification model, in which Knudsen diffusion (in the micropores), as well as pore structure variations due to carbon consumption, were included. However, only one reaction was considered to take place, with CO_2 as a gasifying medium. This model simplifies the reaction network, ignoring the participation of an active carbon species and also the product mass transfer and the reactant accumulation. These simplifications yield an analytical solution, at pseudosteady state conditions.

The model proposed here considers the physical and chemical processes occuring in a gasifying single particle and correlates the predicted results with experimental macroscopic data. An active carbon species is assumed (13) to react in two parallel steps to form a gaseous product or stabilized char (coke). Reactant and product diffuse in and out of the particle while the local micropore structure can vary due to carbon reaction and consumption. The model permits estimation of the local radial distribution of reactant and product concentrations, reaction rates, surface areas and porosities with time. Global properties, such as product yields, surface area and porosity are also calculated, for comparison with the corresponding experimental quantities. The model is applied here to coal hydrogasification, a process which has received less attention compared with steam or CO_2 gasification.

FORMULATION OF THE MODEL

A single spherical lignite or coal particle, of radius r_o, is considered to undergo hydrogasification, after initial rapid devolatilization. During this initial stage, a measurable, uniform pore structure, and an assumed hydrogen profile have developed within the particle. The following assumptions apply to the model formulation:
- Isothermal reaction in a uniform, constant hydrogen atmosphere.

- Constant particle size, with uniform radial pore structure distribution initially (t=0).
- Negligible film diffusion resistance around the particle.
- Predominantly micropore structure for the particle.

Char hydrogasification involves an active carbon species, which, with hydrogen yields methane, or by crosslinking results in coke formation and carbon stabilization:

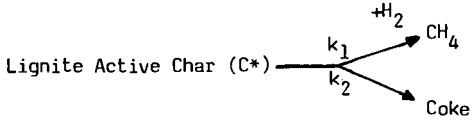

1a)

1b)

From available rate expressions for CH_4 and coke formation (13), the instantaneous, local reaction rates within the particle are given by Equations 2 and 3.

$$R_{CH_4}(r,t) = k_1^o \exp(-\frac{E_1}{RT})\ \rho_p S_g\ C_{C^*} C_{H_2} \qquad 2)$$

$$R_{Coke}(r,t) = k_2^o \exp(-\frac{E_2}{RT})\ \rho_p S_g\ C_{C^*} = \frac{dC_{coke}}{dt} \qquad 3)$$

Reactant (H_2) and product (CH_4) counter diffuse through the porous particle matrix which varies with time and location due to reaction. Thus, the continuity equation for the two gaseous species gives:

$$\frac{\partial C_{H_2}}{\partial t} = \frac{1}{r^2}\frac{\partial}{\partial r}(r^2 D_{e,H_2}\frac{\partial C_{H_2}}{\partial r}) - 2R_{CH_4}(r,t) \qquad 4)$$

$$\frac{\partial C_{CH_4}}{\partial t} = \frac{1}{r^2}\frac{\partial}{\partial r}(r^2 D_{e,CH_4}\frac{\partial C_{CH_4}}{\partial r}) + R_{CH_4}(r,t) \qquad 5)$$

The effective diffusivities ($D_{e,j}$) can be related to the Chapman-Enskog diffusivity (D_{H_2/CH_4}) and the Knudsen diffusivity into the micropores (D_k), (14), by

$$D_{e,j} = (\frac{1}{D_{12}} + \frac{1}{D_k})^{-1}\ \varepsilon^2 \qquad 6)$$

Weight (m) loss and increase of surface area (S_g) and porosity (ε) of the particle occur because of the first reaction, 1a, and, thus, they can be correlated with the conversion to methane (X_{CH_4})

$$\varepsilon = 1 - (1 - X_{CH_4})\ (1 - \varepsilon_o) \qquad 7)$$

$$m = m_o + \frac{4}{3}\pi r^2\ \rho_t(\varepsilon_o - \varepsilon) \qquad 8)$$

$$\rho_p = \rho_t\ (1 - \varepsilon) \qquad 9)$$

Relation 6, between bulk (ρ_p) and true (ρ_t) particle density, is valid for non-swelling or -shrinking particles of constant size. For moderate conversions, the surface area may be assumed to vary linearly with porosity (15)

$$S_g = S_o\ \varepsilon \qquad 10)$$

This system of non-linear partial differential equations was converted to a system of dimensionless non-linear algebraic equations by the explicit finite difference method. Equation 2-4 and 6-10 were solved iteratively, using the Brown technique (16) and the appropriate boundary conditions for C_{C*}, ϵ, C_{H_2} below. Solution of Eq. 5, with the pertinent B.C. for C_{CH_4} below, gives the methane distribution in the particle.

$$\text{At } t = 0 \text{ and } 0 \leq r \leq r_o \qquad \begin{cases} C_{C*} = C_{C_o^*} \\ \epsilon = \epsilon_o \\ X_{CH_4} = 0 \\ X_{coke} = 0 \end{cases}$$

$$t > 0 \text{ and } r = r_o \qquad \begin{cases} C_{H_2} = C_{H_2,S} \\ C_{CH_4} = 0 \end{cases} \qquad 11)$$

$$t > 0 \text{ and } r = 0 \qquad \begin{cases} \frac{\partial C_{H_2}}{\partial r} = 0, \quad \frac{\partial C_{CH_4}}{\partial r} = 0 \end{cases}$$

All char carbon ($C_{C_o^*}$) is considered reactive, as indicated by its complete conversion in high pressure experiments. Since hydrogasification occurs after initial rapid hydropyrolysis (17), some hydrogen profile is expected within the particle matrix. Thus, instead of the conventional boundary conditions for hydrogen, a simple linear initial profile has been assumed and tested

$$\text{At } t = 0 \text{ and } 0 \leq r \leq r_o \qquad C_{H_2} = \frac{r}{r_o} C_{H_2,S} \qquad 12)$$

A linear, or perhaps a parabolic, hydrogen profile should be more realistic, since hydrogen has penetrated into the pores during the first stage. Alternatively, a uniform zero hydrogen concentration may be assumed ($C_{H_2} = 0$ at $t = 0$, $r \leq r_o$), or even a uniform concentration equal to the bulk one ($C_{H_2} = C_{H_2,S}$ at $t = 0$, $r \leq r_o$).

Parameter values were obtained either experimentally or from the literature. Values of k_1^o, E_1, S_o, ϵ_o and ρ_t were measured at 800 - 950°C, while k_2^o and E_2 are experimental values reported in reference (18). The following values were used

E_1 = 35600 cal/mol
E_2 = 28600 cal/mol
k_1^o = 1.7x10^{-6} m^4/mol·min
k_2^o = 3.77x10^{-7} m/min
ρ_t = 1.42 gr/cm^3

S_o^{800} = 355 m^2/g
S_o^{850} = 388 m^2/g
S_o^{900} = 395 m^2/g
S_o^{950} = 410 m^2/g

ϵ_o^{800} = 0.17
ϵ_o^{850} = 0.175
ϵ_o^{900} = 0.18
ϵ_o^{950} = 0.19

EXPERIMENTAL

Lignite hydrogasification experiments, to obtain kinetic parameters and macroscopic, global properties, were performed in a TGA (DuPont 99) system and in an isothermal, tubular reactor (17, 19). Products were continuously analyzed by GC and IR. Pore structure, porosity, density and surface area of lignite chars, at various times and temperatures, were characterized by multipoint BET, helium pycnometry, CO_2 and N_2 adsorption (20).

RESULTS AND DISCUSSION

The model formulated above has been solved using a simple, linear profile for the initial concentration of hydrogen within the particle. Solution has been obtained at eleven radial positions for a time period of 30 min using a time increment of one minute. The results permit estimation of non-measurable quantities, such as the temporal-radial distribution of (a) hydrogen, methane and coke concentration; (b) porosity and surface area; and (c) local rates of methane and coke formation, under various reaction conditions. Integration of predicted results over the whole particle yields global properties, such as particle weight loss, methane yield and rate of formation, total porosity and surface area.

Comparison of predicted and measured macroscopic properties should establish first the adequacy of the model to describe the chemical and physical processes. Figure 1 shows calculated and experimental values of carbon conversion to methane at various times and temperatures. In most cases, agreement is good. Some deviation of experimental data, especially at high temperatures, may arise from a number of reasons, e.g. different initial hydrogen profile, slightly higher order in H_2 for reaction 1a, or higher k_2 and E_2 values than those obtained from the literature for the crosslinking and carbon stabilization reaction.

Similarly, the predicted development of total particle surface area and porosity is in good agreement with the measured physical properties up to 30-40 min, Figures 2 and 3. One should note, here, that Equations 7 - 10 of the model assume a linear growth of surface area and porosity, directly proportional to carbon conversion to methane. Pore blockage, because of carbon stabilization and crosslinking, is not currently considered in the model. This phenomenon may explain the decline of S_g and ε at prolonged times.

After the above macroscopic comparison of model and experimental results, a microscopic examination should unravel the transformations that a lignite particle undergoes during hydrogasification. Figure 4 shows the anticipated hydrogen concentration profile in the particle, at various times. If the initial (t=0) hydrogen concentration is assumed to vary linearly with radius, C_{H_2} in the pores increases with time; however, it always remains less than the bulk one, because of partial consumption of H_2 to form methane and counter-diffusion of the product. The hydrogen concentration in the pores is also expected to increase (albeit somewhat slower) in the case of uniform, zero C_{H_2} initially. If at $t=0$, $C_{H_2}=C_{H_2,S}$, hydrogen diffuses into the pores faster than it reacts and its concentration remains constant with time.

Methane is produced by reaction of active carbon with H_2 and diffuses out of the gasifying particle. Its concentration distribution radially can be predicted by this model, as shown in Figure 5. At the outer layers of the particle, the high local C_{H_2} results in high carbon-to-CH_4 conversion and, thus, methane concentration increases. The decline of CH_4 at the surface ($r=r_o$) is caused by the assumption that methane is so diluted in the bulk stream that its bulk and surface concentration is virtually zero. Methane concentration in the particle increases with time because of C_{H_2} increase, cf. Fig. 4.

Carbon consumption to form gaseous methane should increase the number and size of pores within the particle, dependent on rate. If the "specific surface area", S_g, is used as an approximate, lumped measure of pore structure development, a surface area radial distribution can be predicted, Figure 6. This area increases, from the center of the particle outwards, because of the higher H_2 concentration and rate in the outer shells. Since C_{H_2} increases with time within the particle, S_g also increases, to a substantial difference of ~ 50 m^2/g between surface and center at 30 min reaction time. A similar trend is predicted for the local "porosity", ε, radially with time.

The calculated local values of C_{H_2}, S_g, ε permit estimation of the local reaction rate for methane formation at any time, Figure 7. Rate increases outwards, following a trend analogous to C_{H_2} and S_g. Around the center of the particle, C_{H_2} increase with time results in significant increase of R_{CH_4} after 30 min. Near the surface, R_{CH_4} is affected by the surface area increase (cf. Fig. 6), since C_{H_2} there changes little (Fig. 4).

Figure 7 and Equation 2 indicate that hydrogasification is sensitive to H_2

partial pressure. Thus, recycle of the reactant stream without prior separation of product could affect rates in the pores significantly. Figure 8 shows a drastic decrease of methane formation rate within a gasifying particle, at 5 min. With $P_{CH_4} : P_{H_2} = 1 : 1$ in the bulk stream, rates drop to almost zero for $r < 0.5\ r_o$, and to less than 15 % of that for pure H_2, at r_o. Integration of these curves with location and time show that carbon conversion to methane at 900°C should drop from ~6% in pure H_2 to ~1% at $P_{H_2} = 0.5$ atm.

The model described here takes into account a realistic, two path reaction scheme for hydrogasification, with simultaneous variation of the pore structure properties of the gasifying char particle. Porosity and surface area do not develop uniformly, within the particle, with time and this affects hydrogen penetration, methane counter-diffusion and, thus, the microscopic and global rate of gasification. The model predicts succesfully experimental macroscopic quantities, up to 30-40 min of gasification. Beyond this time, carbon stabilization and pore blockage may cause some deviation. The use of the model can be easily extended to noncaking coals other than lignite and to other gasification media such as CO_2 or steam.

ACNOWLEDGEMENT

The authors wish to thank the European Coal and Steel Community and the Chemical Process Engineering Research Institute of Thessaloniki for financial support of this work.

LIST OF SYMBOLS

C^*	Active carbon concentration (mol/m^3).
C_{CH_4}	Intraparticle methane concentration (mol/m^3).
C_{H_2}	Intraparticle hydrogen concentration (mol/m^3).
$C_{H_2,S}$	Bulk hydrogen concentration (mol/m^3).
$D_{e,j}$	Effective diffusivity of species j (H_2 or CH_4) (m^2/s).
D_{12}	Chapman-Enskog diffusivity (m^2/s).
D_k	Knudsen diffusivity (m^2/s).
E_1, E_2	Activation energies of methane and coke formation (cal/mol).
ϵ	Porosity of particle.
I	Binary diffusivity coefficient (0.25 for D_{e,H_2} and -0.5 for D_{e,CH_4}).
k_1^o, k_2^o	Rate constants of methane and coke formation.
m	Particle mass (g).
ρ_p	Bulk density of particle (g/cm^3).
ρ_t	True density (g/cm^3).
r	Particle radial coordinate (μ).
r_o	Particle radius (μ).
R	Universal gas constant (1.987 cal/mol K).
R_{CH_4} (r,t)	Rate of methane formation (mol/m^3 min).
R_{coke} (r,t)	Rate of coking reaction (mol/m^3 min).
S_g	Specific surface area (m^2/g).
T	Temperature (K).
t	Time (min).
X_{CH_4}	Methane conversion.

Subscripts

o	Initial values at t = 0.
s	Bulk stream and particle surface property.

REFERENCES

1. Moseley F. and Paterson D., J. Inst. Fuel., 38, 13, (1965).
2. Johnson J.L., Adv. Chem. Ser., 131, 145, (1974).
3. Wen C.Y. and Huebler J., Ind. Eng. Chem. Process Des. Dev. 4, 142, (1965).
4. Schmal M., Monterlo J.L.F. and Castellan J.L., Ind. Eng. Chem. Process Des. Dev. 21, 256, (1982).

5. Anthony D.B. and Howard J.B., AIChE J., 22, 625, (1976).
6. Arri L.E. and Amundson N.R., AIChE J., 24, 72, (1978).
7. Russel W.B., Savill D.A. and Greene M.I., AIChE J., 25, 65, (1979).
8. Gavalas R.G. and Wilks K.A., AIChE J., 26, 201, (1980).
9. Bliek A., Poelje W.M., Swaalj W.P.M. and van Beckum F.P.H., AIChE J., 31, 1666 (1985).
10. Shaub G., Peters W.A. and Howard J.B., AIChE J., 31, 903, (1985).
11. Sotirchos S.V. and Amundson N.R., AIChE J., 30, 537, (1984).
12. Lee S., Angus J.C., Edwards R.V. and Gardner N.C., AIChE J., 30, 583, (1984).
13. Zahradnik R.L. and Glenn R.A., Fuel, 50, 77, (1971).
14. Walker Jr., P.L., Rusinko Jr., F. and Austin L.G., Adv. Catal., 11, 133, (1959).
15. Hill, Jr., C.G., "An Introduction to Chemical Engineering Kinetics and Reactor Design" J.Wiley, N.Y. (1977), pp 434.
16. Brown K.M., Comm. ACM, 10, 728, (1967).
17. Kokorotsikos P.S., Stavropoulos G.G. and Sakellaropoulos G.P., Fuel, 65, 1462, (1986).
18. Banerjee D.K., Laidler K.J., Nandi B.N. and Patmore D.J., Fuel, 65, 480, (1986).
19. Kokorotsikos P.S., Stavropoulos G.G. and Sakellaropoulos G.P., Proc. Int. Conf. Coal Sci., 253, Sydney, Oct. 1985.
20. Stavropoulos G.G., Kokorotsikos P.S., Sakellaropoulos G.P., Carbon 86, 4th Int. Carbon Conf., 579, Baden-Baden, July 1986.

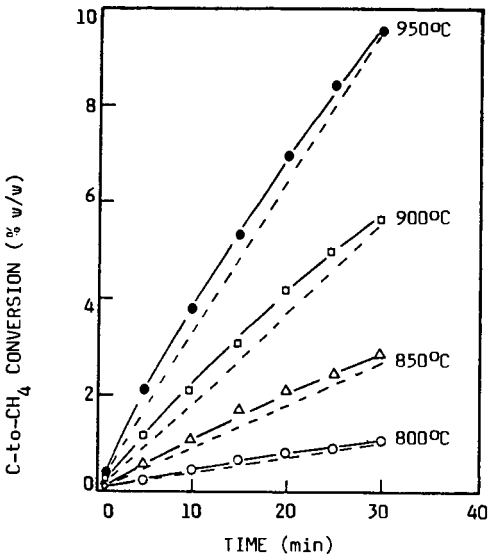

Figure 1. Comparison of model-predicted (dashed) and experimental values for the conversion of char carbon to methane. Points and solid lines are experimental data for hydrogasification.

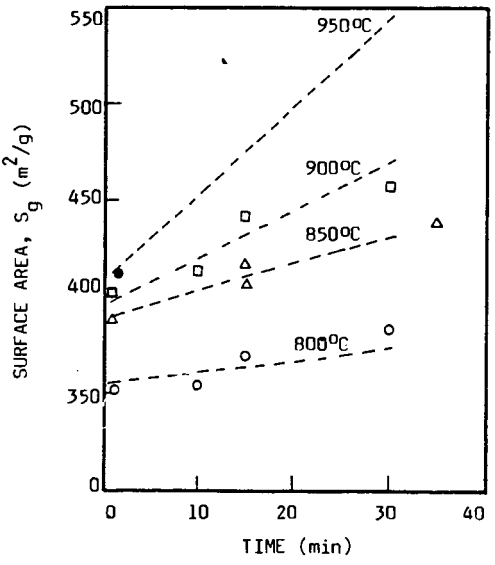

Figure 2. Calculated total surface area (dashed lines) and experimental data (points), compared at various conditions.

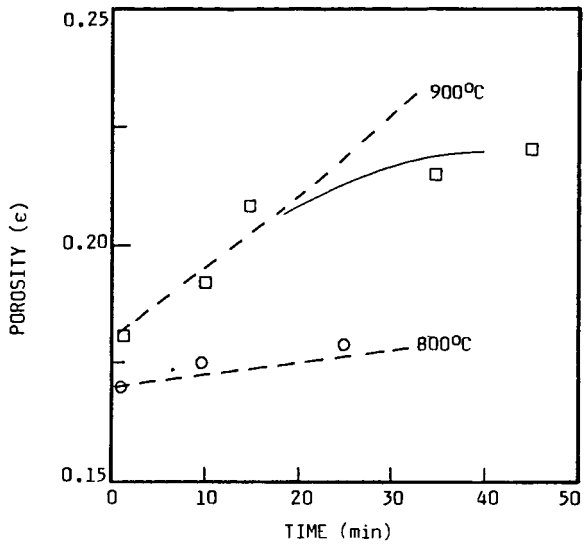

Figure 3. Porosity development of a lignite particle as measured experimentally (points) and predicted by the model (dashed lines).

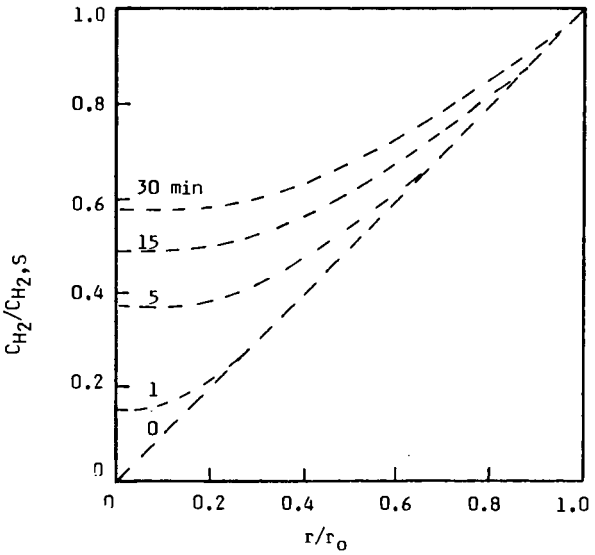

Figure 4. Hydrogen concentration profile with time in a gasifying lignite particle at 900°C (r_o=100μ).

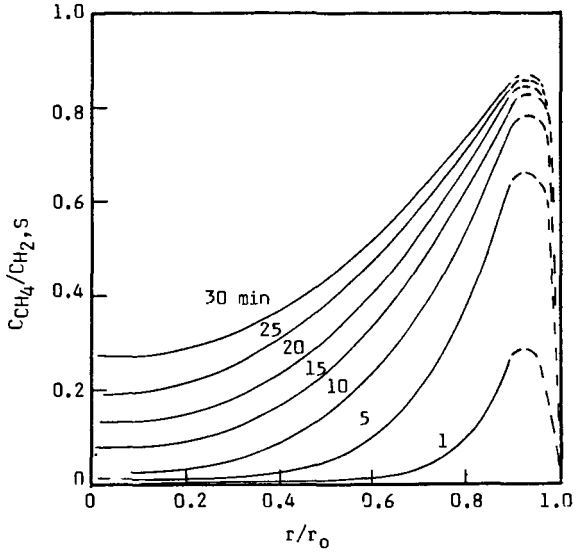

Figure 5. Methane concentration profile with time in a lignite particle at 900°C (r_o≈100μ).

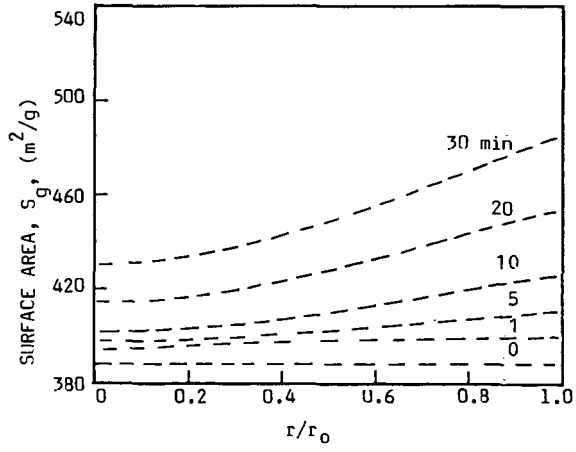

Figure 6. Surface area distribution with time, within a gasifying lignite particle at 900° C (r_o = 100 μ).

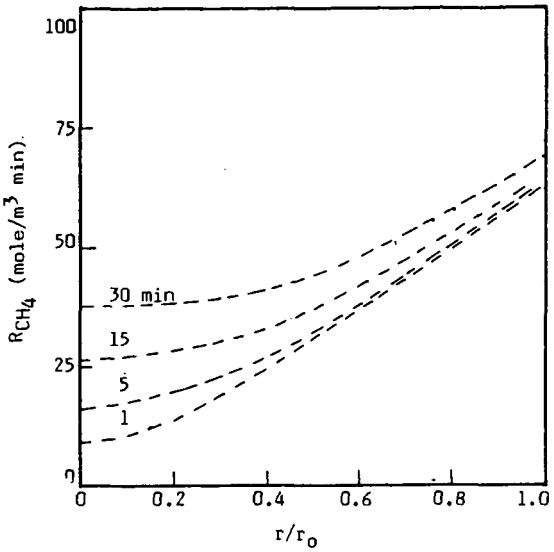

Figure 7. Radial distribution of methane formation with time in a lignite particle at 900°C (r_o = 100μ).

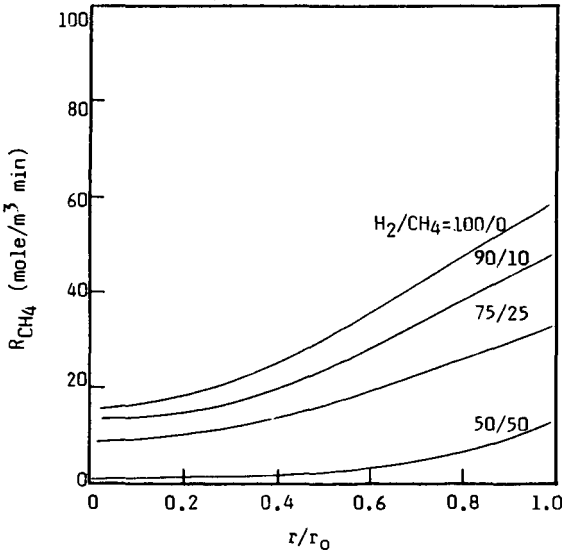

Figure 8. Effect of H_2 partial pressure on the radial distribution of methane formation, at 900°C and 5 min, (r_o = 100 μ).